POLYPUBLIE

The current state-of-the-art of spinal cord imaging: Methods

P. W. Stroman, Claudia Angela M. Gandini Wheeler-Kingshott, M. Bacon, J. M. Schwab, R. Bosma, J. Brooks, D. Cadotte, T. Carlstedt, O. Ciccarelli, Julien Cohen-Adad, A. Curt, N. Evangelou, M. G. Fehlings, M. Filippi, B. J. Kelley, S. Kollias, A. Mackay, C. A. Porro, S. Smith, S. M. Strittmatter, ...

Document en libre accès dans PolyPublie
Open Access document in PolyPublie

Date	2014
Type	Article de revue / Article
Version	Version officielle de l'éditeur / Published version
URL de PolyPublie PolyPublie URL	https://publications.polymtl.ca/3460/
Évaluation par les pairs Peer reviewed	Révisé par les pairs / Refereed
Conditions d'utilisation Terms of use	Creative Commons Attribution-Utilisation non commerciale-Pas d'oeuvre dérivée 4.0 International / Creative Commons Attribution-NonCommercial-NoDerivatives 4.0 International (CC BY-NC-ND)
Référence Citation	Stroman, P. W., Wheeler-Kingshott, C. A. M. G., Bacon, M., Schwab, J. M., Bosma, R., Brooks, J., Cadotte, D., Carlstedt, T., Ciccarelli, O., Cohen-Adad, J., Curt, A., Evangelou, N., Fehlings, M. G., Filippi, M., Kelley, B. J., Kollias, S., Mackay, A., Porro, C. A., Smith, S., ... Tracey, I. (2014). The current state-of-the-art of spinal cord imaging: Methods. NeuroImage, 84, 1070. https://doi.org/10.1016/j.neuroimage.2013.04.124

Publication officielle
Official publication

Titre de la revue Journal title	NeuroImage (vol. 84)
Maison d'édition Publisher	Elsevier
URL officielle Official URL	https://doi.org/10.1016/j.neuroimage.2013.04.124
Mention légale Legal notice	

Ce fichier a été téléchargé à partir de PolyPublie, le dépôt institutionnel de Polytechnique Montréal
This file has been downloaded from PolyPublie, the institutional repository of Polytechnique Montréal
https://publications.polymtl.ca

NeuroImage 84 (2014) 1070–1081

Contents lists available at ScienceDirect

NeuroImage

journal homepage: www.elsevier.com/locate/ynimg

Review

The current state-of-the-art of spinal cord imaging: Methods

P.W. Stroman [a,*], C. Wheeler-Kingshott [b,h], M. Bacon [c], J.M. Schwab [d,e], R. Bosma [a], J. Brooks [f], D. Cadotte [g], T. Carlstedt [b], O. Ciccarelli [b], J. Cohen-Adad [g], A. Curt [i], N. Evangelou [j], M.G. Fehlings [g], M. Filippi [k], B.J. Kelley [l], S. Kollias [m], A. Mackay [n,o], C.A. Porro [p], S. Smith [q], S.M. Strittmatter [l], P. Summers [p], I. Tracey [f]

[a] Centre for Neuroscience Studies, Queen's University, Kingston, ON, Canada
[b] NMR Research Unit, Queen Square MS Centre, UCL Institute of Neurology, London, England, UK
[c] International Spinal Research Trust, Bramley, England, UK
[d] Wings for Life Spinal Cord Research Foundation, Salzburg, Austria
[e] Charité, Universitätsmedizin Berlin, Germany
[f] FMRIB Centre, Nuffield Department Clinical Neurosciences & Nuffield Division Anaesthetics, University of Oxford, England, UK
[g] Division of Neurosurgery and Spinal Program, University of Toronto, Toronto, Ontario, Canada
[h] Institute of Biomedical Engineering, Ecole Polytechnique de Montreal, Montreal, QC, Canada
[i] Balgrist University Hospital, Spinal Cord Injury Center, Zurich, Switzerland
[j] University of Nottingham, Nottingham, UK
[k] Neuroimaging Research Unit, Scientific Institute and University Hospital San Raffaele, Milan, Italy
[l] Biological and Biomedical Sciences, Yale University, New Haven, CT, USA
[m] Institute for Neuroradiology, University Hospital Zurich, Zurich, Switzerland
[n] Dept of Radiology, University of British Columbia, Vancouver, BC, Canada
[o] Dept of Physics & Astronomy, University of British Columbia, Vancouver, BC, Canada
[p] Department of Biomedical, Metabolic and Neural Sciences, University of Modena and Reggio Emilia, Modena, Italy
[q] Vanderbilt University, Institute of Imaging Science, Nashville, TN, USA

ARTICLE INFO

Article history:
Accepted 16 April 2013
Available online 14 May 2013

Keywords:
Magnetic resonance
Positron emission tomography
Spinal cord
Imaging
Spectroscopy
Artifacts
Physiological motion
Susceptibility
Human

ABSTRACT

A first-ever spinal cord imaging meeting was sponsored by the International Spinal Research Trust and the Wings for Life Foundation with the aim of identifying the current state-of-the-art of spinal cord imaging, the current greatest challenges, and greatest needs for future development. This meeting was attended by a small group of invited experts spanning all aspects of spinal cord imaging from basic research to clinical practice. The greatest current challenges for spinal cord imaging were identified as arising from the imaging environment itself; difficult imaging environment created by the bone surrounding the spinal canal, physiological motion of the cord and adjacent tissues, and small cross-sectional dimensions of the spinal cord, exacerbated by metallic implants often present in injured patients. Challenges were also identified as a result of a lack of "critical mass" of researchers taking on the development of spinal cord imaging, affecting both the rate of progress in the field, and the demand for equipment and software to manufacturers to produce the necessary tools. Here we define the current state-of-the-art of spinal cord imaging, discuss the underlying theory and challenges, and present the evidence for the current and potential power of these methods. In two review papers (part I and part II), we propose that the challenges can be overcome with advances in methods, improving availability and effectiveness of methods, and linking existing researchers to create the necessary scientific and clinical network to advance the rate of progress and impact of the research.

© 2013 Elsevier Inc. All rights reserved.

Contents

Introduction . . . 1071
Background . . . 1071
MR methods, challenges and strengths . . . 1071
Inhomogeneous magnetic field . . . 1072
Small cross-sectional dimensions . . . 1072

* Corresponding author at: Centre for Neuroscience Studies, 228 Botterell Hall, 18 Stuart St, Queen's University, Kingston, ON, Canada.
E-mail address: stromanp@queensu.ca (P.W. Stroman).

1053-8119/$ – see front matter © 2013 Elsevier Inc. All rights reserved.
http://dx.doi.org/10.1016/j.neuroimage.2013.04.124

Physiological motion . . . 1072
Current state-of-the-art, and how challenges are being addressed . . . 1072
Functional MRI . . . 1072
Choice of imaging method . . . 1073
Diffusion tensor imaging . . . 1073
Background . . . 1073
Acquisition parameters . . . 1074
DTI in the human spinal cord: methods . . . 1074
Quantifying DTI metrics in the spinal cord . . . 1075
Spinal cord spectroscopy . . . 1075
Myelin water-fraction imaging . . . 1076
Magnetization transfer . . . 1076
Quantification methods . . . 1076
Post-processing and analysis methods to overcome challenges for MRI . . . 1077
Physiological motion . . . 1077
Image distortion and co-registration . . . 1077
Motion correction . . . 1077
Positron-emission tomography (PET) . . . 1078
Future directions . . . 1078
Acknowledgments . . . 1079
Conflict of interest statement . . . 1079
References . . . 1079

Introduction

Non-invasive investigation of human spinal cord function, and the effects of spinal cord injury or disease, is significantly hampered by the inaccessibility of the spinal cord. In order to supplement current methods for assessing residual function, pain, and quality of life factors after spinal cord injury or disease, sensitive methods are needed to reveal changes in neurological function, and structure. Non-invasive imaging methods such as magnetic resonance imaging (MRI), positron emission tomography (PET), and computed tomography (CT), provide the only means of accessing the structure and function of the human spinal cord. As a result, there is currently a great need for development of these methods. While progress is being made, only a relatively small number of research labs in the world are actively working on spinal cord imaging methods, and these techniques have yet to be advanced into clinical use. The potential outcomes of advancing these methods are tremendous, enhancing our basic understanding of healthy human spinal cord function, and impacting our ability to accurately diagnose and treat injury and disease, and predict outcomes. In order to support the development of spinal cord imaging methods and advance the current technology, the objectives of this paper are:

1) to describe the current state-of-the-art of spinal cord imaging by reviewing current methodologies, and
2) to identify the current greatest challenges both innate to spinal cord imaging, and relative to hardware and software development.

This is the first of two papers, and is focussed on spinal cord imaging methods. X-ray based imaging methods such as plain film X-ray and CT demonstrate highly detailed images with contrast between soft tissues and boney structures and are already in routine clinical use for visualizing gross structural changes after trauma to the spine, and diseases of the intervertebral discs. Therefore only PET and MRI methods are described in this paper, with most of the attention on functional MRI (fMRI), diffusion-weighted imaging (DWI) and its extension to diffusion-tensor imaging (DTI), MR imaging based on magnetization transfer and identifying myelin water, and also MR spectroscopy. In a second paper, we will describe the current applications of these spinal cord imaging methods for assessing spinal cord injury, multiple-sclerosis, and pain. The overall goal of this work is to improve tools for spinal cord research and clinical assessments by overcoming the current challenges for imaging and make full use of the potential of these non-invasive methods.

Background

The anatomy of the spinal cord and surrounding structures renders the cord inaccessible for human research, and non-invasive imaging methods are therefore essential. It is also this anatomical arrangement that creates most of the challenges of imaging the spinal cord.

The spinal cord lies within the spinal canal inside the spine, and is surrounded by a variable layer of cerebrospinal fluid (CSF), and then a thick layer of bone or cartilaginous discs between the vertebral bodies. At its widest point of the cervical enlargement it is only ~15 mm across, and has an average length of approximately 45 cm in adult humans (Goto and Otsuka, 1997). The cerebrospinal fluid flows back and forth in the head–foot direction with each heart-beat, with a peak flow speak of roughly 3 cm/s, and with a general progression of movement down one side of the spinal cord and up the other (Feinberg and Mark, 1987; Matsuzaki et al., 1996). The pulsating CSF flow, and possibly arterial pulsation as well, cause the spinal cord to move within the spinal canal, with an amplitude that diminishes with greater distance from the head (Figley and Stroman, 2006, 2007). Given that the spinal cord ends at around the 12th thoracic vertebra (the exact location varies between individuals), the entire cord is relatively close to the heart and lungs.

The anatomical arrangement of the spinal cord is reversed from that of the brain, with the gray matter (largely nerve cell bodies, glial cells, and interneurons) within a characteristic butterfly-shape cross-section at the center of the cord, surrounded by white matter tracts. The main arteries supplying the cord lie along the cord surface, one above the anterior median fissure and two along the posterior side of the cord, and these are connected by lateral branches (Thron, 1988). The anterior artery sends branches into the anterior median fissure with further branching to supply the gray matter from the center outward. Venules and small veins carry blood radially from the gray matter to the cord surface.

MR methods, challenges and strengths

Imaging of the spinal cord presents inherent challenges that are common to all MR imaging and spectroscopy applications. Specifically, these are 1) the spatially non-uniform (inhomogeneous) magnetic field environment when in an MRI system, 2) the small physical dimensions of the cord cross-section, and 3) physiological motion. For non-MRI applications, such as PET and SPECT, the latter two of these challenges also apply. Here we discuss these key challenges for spinal

cord imaging, and describe their characteristics, and methods that have been developed to overcome these challenges both generally, and in later sections, for specific methods such as fMRI, DTI, anatomical imaging, and spectroscopy.

Inhomogeneous magnetic field

The greatest challenge for acquiring MR images in the spinal cord is the inhomogeneous magnetic field in this region. Differences in magnetic susceptibility between bone, soft tissues, and air, result in image distortion and a loss of signal intensity. In this respect, the spinal cord is one of the worst environments for using MR in the human body. Most current MRI systems provide the option of shimming the magnetic field (i.e., making the field more uniform), for each volume of the body to be scanned, and increasingly, the ability to optimize the shimming only within the spinal cord. However, while volume shimming improves the field homogeneity, it is limited to smooth variations across space and cannot fully compensate for small, localized, field variations, such as at cartilaginous discs between vertebral bodies.

The geometry of the field inhomogeneity must be considered in order to avoid its effects. Images obtained transverse to the spine can provide better image quality than sagittal or coronal slices, because there is less field variation across the slice thickness. This is particularly effective when the slices are aligned with either the intervertebral discs or the centers of the vertebral bodies (Stroman and Ryner, 2001), but this choice of slice orientation and positioning can limit the anatomical coverage of the images.

The image quality can be further optimized by a suitable choice of pulse sequence. With few exceptions, MR imaging methods are either based on a gradient-echo, or a spin echo pulse sequence. As echo times increase, these sequences become progressively T_2^*- and T_2-weighted respectively. The key difference between them is that the spin-echo employs a refocusing pulse (typically producing a 180° rotation of the magnetization in the tissues) in order to reverse the effects of static field inhomogeneity for a brief instant of time. The MR signal at the peak of the spin-echo is effectively free of the deleterious effects of the inhomogeneous magnetic field, and thus spin-echo imaging provides significant advantages for imaging the spinal cord. Nonetheless, there are situations, as described in later sections, in which either T_2^*-weighting or faster data acquisition is desired in spite of the disadvantages of gradient echo acquisitions.

Small cross-sectional dimensions

The second challenge for MRI of the spinal cord arises from its small physical dimensions. To reliably depict anatomical details, an in-plane spatial resolution of 1 mm × 1 mm, and relatively thin imaging slices (1–2 mm) is fairly typical in many spinal cord applications of MR. Imaging slices transverse to the spinal cord anatomy is therefore favorable for several reasons. First, this orientation places the highest spatial resolution in the plane of the spinal cord cross-section, where the anatomy is more varied, and the greatest resolution is needed. It also allows the choice of phase-encoding in the right/left direction, so that motion artifacts from the heart, lungs, throat, etc. do not spread across the spinal cord in the resulting images. With a right–left phase encoding direction however, the field-of-view must either span the full width of the body, or spatial suppression pulses must be applied to eliminate the signal from regions outside the FOV. Otherwise, aliasing will occur and the shoulders and arms will appear to wrap around inside the image, potentially obscuring the spinal cord. An unavoidable disadvantage of axial slices is that a large number of imaging slices need to be acquired to view a large rostral–caudal extent of the cord, and this can be time consuming.

The natural alternative to axial slices is to use sagittal slices to take advantage of the small dimensions and typically low curvature of the spinal cord in the right–left direction. The anterior–posterior dimensions of the chest are typically much smaller than the right–left dimensions, and aliasing is more easily avoided with sagittal slices. Spatial suppression pulses can be applied anterior to the spine in order to reduce the effects of motion artifacts from the heart, lungs, throat, etc.

Physiological motion

MR imaging of the spinal cord is hampered by the fact that the spinal cord moves within the spinal canal together with the flow of cerebrospinal fluid (CSF). As described above, the pulsation of CSF flow diminishes with distance away from the head, and correspondingly the lumbar spinal cord moves very little, if at all (Figley and Stroman, 2006, 2007). In addition, the entire spine can move slightly with respiration, depending on posture, and, as mentioned above, the entire spinal cord is near the heart, lungs, and visceral organs which also undergo periodic movements.

The effects of periodic physiological motion can be reduced or even eliminated by synchronizing the acquisition with the cardiac and respiratory cycles (i.e., "gating"). The drawbacks of this method are that it can increase the acquisition time by a factor of 2 or 3 times, and can result in a variable repetition time (TR).

Image artifacts produced by motion are distributed across the image in the phase-encoding direction. Thus, choosing the phase encoding direction such that artifacts do not spread across the spinal cord from the CSF, heart, or lungs, can improve spinal cord depiction in the resulting images. "Motion compensating" gradients and averaging the signal across multiple phases of motion can also be applied to reduce motion artifacts. In the specific case of functional MRI, however, signal averaging and gating are not practical options because of the loss of temporal resolution and potential for variable T_1-weighting if TR values vary.

Current state-of-the-art, and how challenges are being addressed

Functional MRI

In functional MRI, anatomical images are acquired quickly and repeatedly over time in order to detect changes corresponding to tasks or sensory stimuli. Subtle changes can be detected in these images as a result of the coupling between the supply of oxygenated blood and metabolic demand of the tissues. Oxygenated hemoglobin has different magnetic properties than de-oxygenated hemoglobin and therefore behaves as an endogenous MR contrast agent related to the amount of oxygen being carried by the blood. The MR signal relaxation times (T_2 and T_2^*), and consequently the image signal intensity, therefore vary subtly between regions, depending on the metabolic activity, with blood oxygenation-level dependent (BOLD) contrast.

The use of fMRI in the spinal cord has required adaptation from the methods that are well-established for brain fMRI in order to address the challenges discussed above. Some of the earliest papers published on functional MRI of the spinal cord sought to address the technical challenges, and to confirm that the BOLD contrast mechanism could indeed be detected in the spinal cord (Stroman and Ryner, 2001). To this end, fMRI data were acquired with both spin-echo and gradient-echo imaging methods. This allowed comparisons to be made with previous brain fMRI studies which showed that signal changes with BOLD contrast are roughly 3.5 times larger with T_2^*-weighted imaging than with T_2-weighting, at the same echo time. While both imaging methods demonstrated signal changes in the spinal cord during the performance of a one-hand motor task, and with a sensory stimulus, the magnitudes of the responses with T_2^*- and T_2-weighted imaging methods were similar at roughly 5–6%. The conclusions from this paper were that the BOLD response had been detected in the spinal cord, and a series of studies followed investigating the apparent departure from the known properties of BOLD (Figley et al., 2010; Figley and Stroman, 2011; Jochimsen et al., 2005; Stroman et al., 2001a,b, 2002, 2003a,b, 2005, 2008). The primary outcome of these studies was the proposal of a second MRI contrast mechanism that occurs due to changes in

tissue water content, termed "signal enhancement by extravascular water protons", or "SEEP". The higher BOLD sensitivity of gradient-echo methods was also found to be offset by lower image quality and signal-to-noise ratio than can be obtained with spin-echo imaging of the spinal cord. This established spin-echo methods as a suitable option for spinal cord fMRI.

The distinction between gradient-echo and spin-echo methods has particular relevance in the spinal cord because the superficial draining veins are separated from the gray matter of the spinal cord by the white matter tracts. It has been well-recognized in brain fMRI studies that gradient echo sequences are sensitive to BOLD changes in these veins and so may be prone to dissociation between the site of signal change and the site of neuronal activity (Bandettini et al., 1994; Gati et al., 1997). This is given further support by a hypercapnia challenge study that showed the gradient echo BOLD response to be dominated by signal changes at the spinal cord surface (Cohen-Adad et al., 2010). While masking to include only the spinal cord can be used to avoid this effect, spin-echo scans are intrinsically less sensitive to the contribution from draining veins and therefore may provide greater spatial precision for detecting neural activity (Bandettini et al., 1994; Gati et al., 1997).

Choice of imaging method

For functional MRI of the spinal cord, as with any fMRI method, fast imaging is essential, but the echo-planar spatial encoding schemes, typically used for brain fMRI, are highly prone to distortions in and around the spinal cord due to magnetic field inhomogeneities (Fig. 1). Fast spin-echo schemes on the other hand, in particular the single-shot fast spin-echo, can produce images relatively free of distortion while maintaining a short acquisition time. For this reason, the majority of spinal cord fMRI studies carried out to date have employed spin-echo imaging methods.

The fast spin-echo has one drawback for fMRI due to the large number of radio-frequency (RF) refocusing pulses (typically 180° pulses) that must be applied to create a train of spin-echoes (Stroman, 2010). The amount of energy that is deposited in the tissues (the specific absorption ratio, SAR) can exceed acceptable levels, particularly at higher field strengths. Partial-Fourier acquisitions are an option to reduce the number of RF pulses that need to be applied, and therefore reduce the energy deposition and the acquisition time. However, partial-Fourier acquisitions can be more sensitive to motion artifacts and have a lower signal-to-noise ratio (SNR) due to the lower number of data points sampled to produce the image (Murphy et al., 2007). In order to deposit less energy, an alternative is to use lower flip angle pulses for refocusing. Again, the trade-off is lower SNR, but without the expense of more sensitivity to motion. Longer TE values provide the advantage of enabling acquisition of more lines of data on both sides of the center of k-space which contributes to improving the SNR, and can help reduce sensitivity to motion (Stroman, 2010). The theoretical optimal TE for BOLD contrast with spin-echo scans would equal the T_2 value of the tissues (approximately 75 ms) or the T_2^* (~30 ms at 3 T) for gradient echo scans (Smith et al., 2008). Accordingly, a recent study (Stroman et al., 2012a) indicates that spin-echo BOLD fMRI with TE = 75 ms may provide the optimal combination of sensitivity and contrast for spinal fMRI. Limitations on the minimum TE typically result in a pure SEEP contrast being unachievable for single-shot fast spin-echo acquisitions. The TE value that will provide the highest sensitivity for a combination of BOLD and SEEP contrast in spinal fMRI is, as yet however, undetermined. In practice, the echo time in most published reports is greater than 30 ms with the partial-Fourier single-shot fast spin-echo, resulting in a combination of BOLD and SEEP contrast (Fig. 2).

To summarize (including the methods described in the section MR methods, challenges and strengths), for the purposes of studying the effects of spinal cord injury or disease the optimal parameters appear to be those listed in Table 1.

Diffusion tensor imaging

Background

Conventional MRI exploits interactions between protons in water and their molecular environments which modulate relaxation times, and therefore the MRI signal intensity, to provide image contrast that is useful for detecting pathological changes. In fibrous structures such as the white matter or muscles, water will diffuse further along the fibrous structure than across it, in a given interval of time. In the spinal cord, the microstructure is highly organized and anisotropic, particularly for the white matter tracts that consist of tightly packed bundles of myelinated axons running largely in the rostral–caudal direction. The MRI signal can be made to be sensitive to the slight displacement of water as a result of diffusion by means of strong linear gradients in the magnetic field (Stejskal and Tanner, 1965). An MR image that has been sensitized to water diffusion in this manner can provide information about the microstructural composition of tissues (Horsfield and Jones, 2002). Indices calculated from diffusion MRI experiments (mean diffusivity, axial and radial diffusivity, and fractional anisotropy) have been reported to be sensitive to changes in microstructural integrity, demyelination, axonal loss, and inflammation. We are now in a phase of discovery as to how diffusion experiments performed in the spinal cord can provide a deeper understanding of the changes to tissue structure in a variety of diseases and syndromes.

Methods for encoding diffusion sensitivity into the MRI signal have been well-developed for studying the brain, and the same principles apply for imaging the spinal cord (Beaulieu, 2002; Stejskal and Tanner, 1965). Key concepts are that magnetic field gradients are applied to induce diffusion sensitivity in a specific direction for each

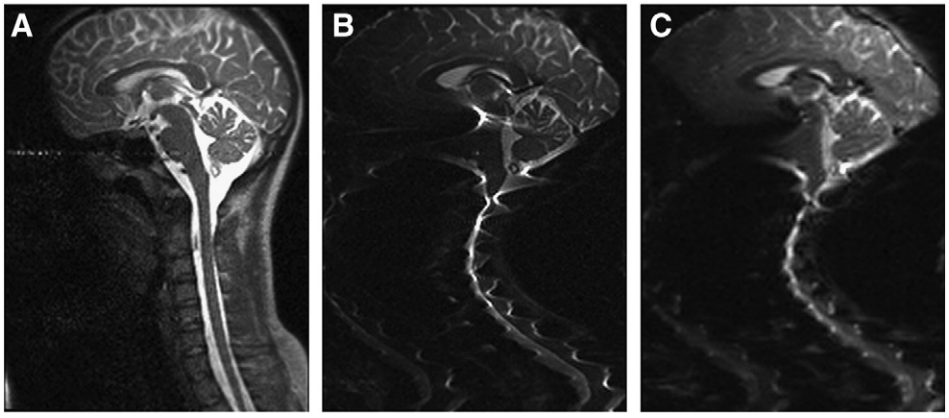


Fig. 1. Spatial distortions caused by bone/tissue interfaces in the spine with A) a half-Fourier single-shot fast spin-echo (HASTE), B) a spin-echo EPI, and C) a gradient-echo EPI imaging sequence.

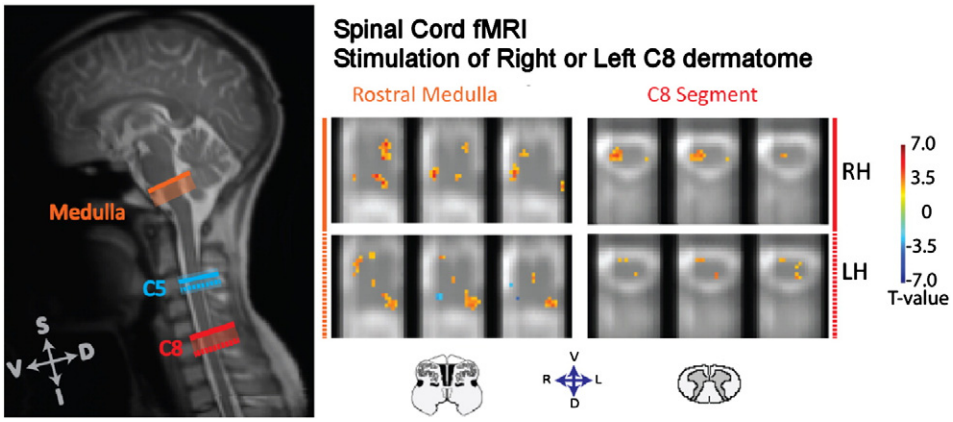


Fig. 2. An example of spinal cord and brainstem fMRI results obtained from a group of healthy participants, with thermal stimulation of the right and left hands. The left panel shows the approximate rostral–caudal locations of the axial slices on the right side of the figure. Results are shown for selected contiguous 1-mm thick transverse slices through the C8 spinal cord segment and the rostral medulla. Areas of activity are displayed in axial slices from spatially normalized functional MRI data, with colors corresponding to the T-value determined with a GLM analysis. The results are shown separately for analyses with paradigms corresponding to right-hand stimulation and left-hand stimulation, and demonstrate spatial specificity.

measurement, with the degree of diffusion sensitivity characterized by the "b" value. The diffusion-weighted MR signal can be expressed as (Stejskal and Tanner, 1965):

$$\frac{S}{S_0} = e^{-bD} \quad (1)$$

where S and S_0 are the signals obtained with and without applied diffusion gradients, respectively, and D is the diffusion constant, also called the apparent diffusion constant (ADC). There are three main types of diffusion experiments: 1) apparent diffusion coefficient (ADC) imaging, 2) diffusion tensor imaging (DTI), and 3) q-space. It should be pointed out, however, that other advanced methods exist (Q-ball, diffusion spectrum imaging, kurtosis), but are beyond the scope of this manuscript. Here, we focus on DTI as it is the most widely used approach in the spinal cord, where the technical complexity of advanced methods increases compared to the brain.

Acquisition parameters

By acquiring MR images with diffusion-weighting applied in each of several directions, it is possible to compute a parametric model representing the main diffusion direction for each voxel (Basser and Pierpaoli, 1996). This model is described by a tensor (3 × 3 matrix) and is usually represented graphically as a 3D ellipsoid. To estimate the diffusion tensor, at least 6 diffusion measurements must be acquired along non-coplanar directions at a given b-value (typically between 700 and 1500 s/mm^2). One measurement at a very low b-value (0–100 s/mm^2) is also required (S_0 in Eq. (1)). From an estimate of the diffusion tensor, it is possible to estimate the amount of diffusion, and the directions, along three principal axes. The direction of greatest diffusion is defined as the primary axis, and is also called the "principal eigenvector", or "PEV". The direction of the PEV is typically related to the primary orientation of the fibers within the voxel. In conjunction with the FA, this value serves as the basis for many fiber tractography algorithms that attempt to reconstruct white matter pathways (Fig. 3) (Jones et al., 2002).

DTI in the human spinal cord: methods

Although widely applied to the brain, acquiring diffusion-weighted images (DWI) of the spinal cord presents the same challenges as other MR methods as listed above. Physiological motion may bias ADC estimation (Kharbanda et al., 2006) and create ghosting artifacts (Clark et al., 2000). The small physical dimensions of the cord contribute to partial volume effects, which are accentuated in the cord by the proximity of white matter tracts to the surrounding cerebrospinal fluid (CSF) (Nunes et al., 2005). As with typical brain fMRI methods, standard DWI and DTI imaging sequences are based on echo-planar imaging (EPI), and are very sensitive to the poor magnetic field homogeneity in the spinal cord (Heidemann et al., 2003).

Although sagittal slices have been employed for DTI studies (Bammer et al., 2002; Cercignani et al., 2003; Jeong et al., 2005; Kharbanda et al., 2006; Shen et al., 2007; Spuentrup et al., 2003; Thurnher and Bammer, 2006), axial DTI of the spinal cord is generally favored as it can reveal more detailed information about specific fiber bundles (Cohen-Adad et al., 2011a; Ellingson et al., 2008; Elshafiey et al., 2002; Gullapalli et al., 2006; Holder et al., 2000; Kim et al., 2007; Klawiter et al., 2011; Madi et al., 2005; Nevo et al., 2001; Ohgiya et al., 2007; Schwartz et al., 1999; Smith et al., 2010; Wheeler-Kingshott et al., 2002a; Wilm et al., 2009). Given the small cross-sectional size and cylindrical geometry of the spinal cord, most DTI studies have employed voxels that are elongated along the spinal cord, with higher in-plane resolution (e.g. 1 × 1 × 5 mm^3). However, this is sub-optimal for tractography studies where isotropic voxels (e.g. 2 × 2 × 2 mm^3) are preferred (Jones et al., 2002).

Table 1
Summary of imaging parameters used for spinal cord fMRI.

Imaging method	Single-shot fast spin-echo (also called SSFSE, HASTE, or SShTSE, depending on the manufacturer)	Gradient-echo EPI
Spatial resolution	1.5 mm × 1.5 mm × 2 mm Contiguous slices	1.5 mm × 1.5 mm × 5 mm Contiguous or spaced to vertebral bodies
Orientation	Sagittal	Axial
Echo time, TE	Minimum possible for SEEP (<20 ms) Moderate for a combination of BOLD and SEEP (~30–40 ms) Longer to optimize contrast from BOLD (~75 ms predicted from theory)	25–40 ms
Repetition time, TR	Longest practical, considering the temporal resolution needed for fMRI	<3 s
Receiver bandwidth	Balance speed and SNR (typical values: 790 Hz/pixel or about 150 kHz)	Highest possible
Imaging options	Flow compensation in H/F direction, Spatial suppression pulses to eliminate signal anterior to the spine Acquire as many phase-encoded lines as possible in the available time and SAR constraints	Flow compensation in H/F direction Spatial suppression pulses to eliminate aliasing Localized shimming

SSFSE: single-shot fast spin-echo, HASTE: half-Fourier single-shot turbo spin-echo, SShTSE: single-shot turbo spin-echo.

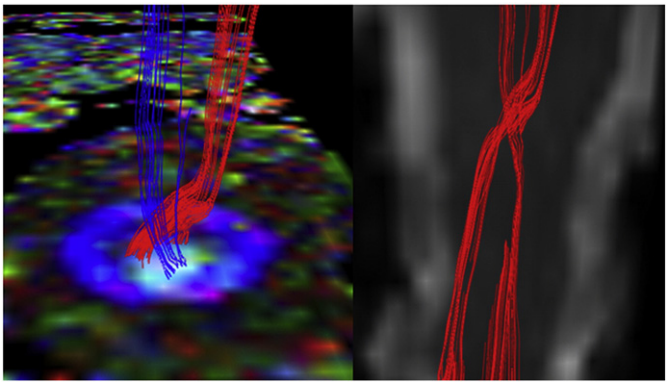


Fig. 3. The panel on the left shows a color-coded representation of diffusion parameters in an axial plane through the level of the medulla oblongata, as well as a selective reconstruction of the corticospinal tracts in a healthy participant. The panel on the right shows the reconstructed fiber tracts overlaid on a sagittal reference image. The decussation of the corticospinal tracts in the medulla is clearly identified in this example.

The optimal b-value varies, depending on the tissues or pathology being studied, available gradient strength, and echo time achievable on each scanner. For example, to achieve a certain b-value (e.g. 700 s/mm^2) older scanners with a maximum gradient strength of 22 mT m^{-1} must apply diffusion-sensitizing gradients for almost twice the duration needed in modern scanners equipped with 40 mT m^{-1} gradient sets. Using lower diffusion weightings has the advantage of a shorter echo time (TE) and therefore an increased SNR. Higher b-values (>1000 s/mm^2) provide more sensitivity for distinguishing degrees of restricted diffusion, and therefore more sensitivity to directional diffusion in white matter fibers, and are recommended when possible to probe microstructure. A balance therefore needs to be struck between diffusion sensitivity and SNR.

The recommended number of directions for robust DTI estimation is at least 20 icosahedral directions (Jones, 2004). The recommended ratio between non-diffusion-weighted data (b = 0) and diffusion-weighted data is 1/8 (Jones et al., 1999). We note that while these numbers result from optimization studies done in the brain and are easily transposed to spinal cord imaging, some studies have argued that the axial symmetry of the cord allows for imaging with a reduced number of directions (Gulani et al., 1997; Schwartz et al., 2005).

Quantifying DTI metrics in the spinal cord

Tractography-based quantification consists of first reconstructing the underlying fiber bundles via tractography algorithms (as implemented in MedINRIA, Diffusion Toolkit, MRIStudio, Camino, FSL, etc.) (Fig. 3). Once the tracts are reconstructed, the DTI metrics within the tracts can be quantified (i.e., within the voxels that include the tracts) (Van Hecke et al., 2008). It is possible to pre-define seed points in various regions of the spinal cord for selective tract generation, and so quantify metrics in specific segments of the spinal cord (Ciccarelli et al., 2007; Cohen-Adad et al., 2011b). Tractography-based quantification is attractive because it can be relatively fast as tractography is a semi-automatic procedure; and it has relatively low operator bias. However, it requires data acquisition that is optimized for tractography, which is typically in a sagittal orientation with isotropic voxels, at the expense of cross-sectional resolution. Substantial inaccuracies can also occur due to partial volume effects, such as near nerve roots and in gray matter regions, or due to residual susceptibility distortions and pathological conditions (Cohen-Adad et al., 2009; Mohamed et al., 2011). An alternative approach is to use ROI-based quantification based on manually drawn ROIs to probe the integrity of specific tracts (Ciccarelli et al., 2007; Cohen-Adad et al., 2008; Klawiter et al., 2011; Lindberg et al., 2010; Onu et al., 2010; Qian et al., 2011). Advantages of this approach include better accuracy, because it requires the user to assess the quality of the ROI, and it can be performed on axial acquisitions with large gaps thereby providing high in-plane resolution. Conversely, the process is time-consuming and open to operator bias.

Spinal cord spectroscopy

Proton MR spectroscopy (MRS) provides useful information about the metabolic and biochemical status of a brain or spinal cord region by quantifying the concentrations of certain metabolites. As these represent potential surrogate markers for the underlying pathological processes, spinal cord MRS may provide information about the extent of pathological involvement in patients with spinal cord injury, not quantifiable with conventional imaging. The metabolite that has been studied (and quantified) most in the spinal cord is N-Acetyl-aspartate (or total NAA, usually equal to NAA + NAA-glutamate) that, despite controversy about its metabolic and neurochemical functions, is one of the most specific in-vivo markers for neuronal health and integrity (Moffett et al., 2007).

Studies using spinal cord MRS have been carried out at 1.5, 2 and 3 T, and have demonstrated that this technique is feasible and that metabolite concentrations in the upper cervical cord can be quantified. The signal from the metabolites is particularly small and so loss of coherence due to magnetic field inhomogeneities, physiological and macroscopic motion, and the small voxel size needed to avoid partial volume effects, all contribute to making spinal cord MRS technically challenging. It is not surprising therefore, that reports on spinal cord MRS of healthy controls (Gomez-Anson et al., 2000; Marliani et al., 2007) and patients with cord tumors, multiple sclerosis, chronic cervical spondylotic myelopathy, chronic whiplash and spinal cord injury (Elliott et al., 2012; Ciccarelli et al., 2007; Holly et al., 2009; Kachramanoglou et al., 2013) have been scarce compared with brain MRS studies.

From a methodological perspective, optimized protocols for quantitative, single voxel 1H-MRS have been shown to provide reliable spectra especially for voxels placed in the upper cervical cord (Cooke et al., 2004). In general, voxels with a volume of about 2 ml and located between C1–C3 (Ciccarelli et al., 2007, 2010) and C2–C3 (Marliani et al., 2007, 2010) have been used, although voxels positioned between C3 and C7 (Kendi et al., 2004) and between C6 and C7 (Henning et al., 2008), have been used. MRS in the lower cervical and thoracic cord is technically very difficult because receiver coils are generally less sensitive to these regions, the spinal cord is smaller, and the amount of vertebral bone is increased, causing further field inhomogeneities that make shimming challenging. In fact, only one study of the lower and thoracic cord has been reported and this made use of an optimized acquisition protocol, which included inner-volume saturated point-resolved spectroscopy sequence (PRESS) localization and advanced (or higher-order) shimming (Henning et al., 2008).

A limitation of single-voxel MRS is that it provides little information on the spatial distribution of metabolites in the spinal cord. Improvement on this method is possible through the use of spectroscopic imaging (MRSI) techniques. For example, 1D PRESS spectroscopy (1D-MRSI) has been used to selectively excite signal in five voxels extending from the pontomedullary junction to the level of the C3 vertebra (Edden et al., 2007). Two-dimensional (2D)-MRSI of water and lipids in the spinal cord has been described (Lin et al., 2000), but so far no study has been published with water-suppressed 2D-MRSI as is needed for detection and quantification of metabolites.

Recent developments at higher field strength (3 T) indicate the possibility to detect additional metabolite concentrations with spinal cord MRS, such as the glutamate/glutamine (Solanky ISMRM 2012). This has been possible with thanks to careful optimization of the acquisition protocol and positioning of the voxel of interest, the use of a cervical collar that reduces the macroscopic movement of the neck, triggered iterative shimming and optimized water suppression.

Myelin water-fraction imaging

The various tissue environments that contribute to the MRI signal can be investigated based on their relaxation times (T_1 and T_2) in order to gain information about tissue changes at the cellular level. Detailed relaxation time studies of excised neural tissues (Whittall et al., 1997) have distinguished three specific relaxation components. These have been identified as CSF, intracellular and extracellular water, and water trapped in myelin sheaths. Within each of these three components there are further sub-environments, but their relaxation times are too similar to be identified separately. In gray matter and white matter in the brain, the two main components are attributed to myelin water with a T_2 of around 15 ms, and the other is attributed to intracellular and extracellular water with a T_2 of approximately 80 ms. The difference is that gray matter derives roughly 3% of its signal from the faster relaxing component ($T_2 \approx 15$ ms) whereas about 11% of white matter signal comes from this component (Jones et al., 2004; Whittall et al., 1997).

The myelin water fraction, MWF, which represents the fraction of tissue water bound to the myelin sheath (Whittall et al., 1997), is a validated marker for myelination in central nervous system tissue in vivo (Laule et al., 2006). MWFs from normal spinal cord are larger than those measured from normal brain and have been found to decrease slightly with age (MacMillan et al., 2011; Wu et al., 2006). Two separate studies (Laule et al., 2010; Wu et al., 2006), have found a lower MWF in the cervical spine of MS patients than in healthy controls. In a longitudinal study on subjects with primary progressive MS (Laule et al., 2010), MWF in the cervical spine was found to decline by 5% per year. Myelin water fraction imaging is a promising technique for the study of spinal cord changes in MS because it provides specific information about the myelination state of the tissue.

Magnetization transfer

Conventional MRI of the spinal cord focuses on T_1 and T_2-weighted (and variants such as the MPRAGE, STIR, and FLAIR) methods because these can reflect tissue changes such as inflammation, necrosis, atrophy and lesions. However, within tissue, there are protons associated with large macromolecules with extremely short T_2 relaxation times (ms); too short to be imaged directly with T_1- and T_2-weighted MRI. However, these semi-solid protons communicate with surrounding bulk water and thus can be interrogated indirectly. Magnetization transfer (MT) is an umbrella term describing this communication, which can occur through dipole–dipole interactions, or direct chemical exchange (Henkelman et al., 2001). While the MT effect can be seen with different pulse sequences, for brevity we will focus on the off-resonance saturation approach (Sled and Pike, 2000, 2001). Because the semi-solid protons have very short T_2 values, their frequency distributions are broad (~100 ppm). Thus, an RF irradiation at a frequency far from the water resonance can selectively saturate these protons without direct saturation of the water. Through spin diffusion and intra-/intermolecular energy exchange, the saturation is transferred to the surrounding water and results in observable signal attenuation (Graham and Henkelman, 1997). As a result, the MT effect is proportional to the relative amounts of water associated with macromolecules and in bulk water, and is therefore different in tissues and in CSF, and has been shown to be sensitive to the myelin concentration, including both loss and regeneration (Brown et al., 2012; McCreary et al., 2009; Schmierer et al., 2004, 2007; Stanisz et al., 2005).

There are two global challenges to saturation-based MT experiments. First, in addition to the sensitivity to macromolecular protons, the MT effect is also sensitive to relaxation times (T_1 and T_2) of the two compartments, B_0 and B_1 field strengths, the amount of direct water saturation, and sequence parameters such as the duty cycle, and the amplitude, power, and bandwidth of the saturation pulse(s). Secondly, saturation-based MT experiments generally require either large saturation powers (>10 mT) or long RF pulses/pulse trains to generate a significant MT effect. Even at lower field strengths, the power deposition (or specific absorption rate, SAR) with body coil transmission is already near the limit for human studies, as specified by the Food and Drug Administration (FDA) in the United States. With the known benefits of higher field strengths, transitioning MT experiments to higher fields quadratically increases power deposition. However, at high field, the prolongation of T_1 values can be utilized to minimize the SAR ($SAR \sim B_0^2(t_{sat}/TR)$) by reducing the duty cycle (Smith et al., 2006). Since the benefit of increasing the TR linearly scales the SAR, while the increase in B_0 has a quadratic relationship, attention has been turned to alternative methods for exploring MT at ultra-high field strengths, such as 7 T (Dortch et al., 2013; Mougin et al., 2010).

Quantification methods

The most prevalent method to quantify the MT effect is by using the magnetization transfer ratio (MTR) (Wolff and Balaban, 1989) where the MTR is defined as:

$$MTR(\Delta\omega) = 1 - \frac{S(\Delta\omega)}{S_0} \tag{2}$$

and $S(\Delta\omega)$ and (S_0) are the signals obtained in the presence or absence of an MT pre-pulse at offset frequency = $\Delta\omega$. The benefit of the MTR is that it removes the dependence on non-MT-based sequence parameters such as the TR, TE, type of imaging sequence, etc. Additionally, the MTR minimizes sensitivity to T_1, T_2, and receiver gain over the length of the anatomy of interest. With this definition, white matter (WM) is bright, gray matter (GM) is less bright, and CSF is minimal with the dynamic range of the MTR being from 0 (no saturation), to 1 (full saturation). One of the appeals of the MTR is the simple nature of the acquisition and analysis, along with the speed with which each acquisition can be obtained.

However, there are potential drawbacks of MTR imaging in the spinal cord. First, because two images are required to determine the MTR, motion between the acquisitions must be corrected. In the spinal cord, high resolution is necessary, and thus motion becomes a significant challenge when calculating the MTR. Because conventional saturation-based MT experiments rely on the build-up of steady-state saturation, triggering methods such as cardiac or respiratory gating cannot be used, as the TR between the two acquisitions must remain constant. Secondly, the MTR is only pseudo-quantitative. That is, the MTR is only a relative measure of saturation, which can vary from vendor to vendor, across field strengths, and with different B_0 shimming routines. Finally, since it is a ratio image, the SNR is decreased relative to a single acquisition method.

An alternative method, termed MTCSF, that is based on a single image, has been reported to overcome the SNR penalty and sensitivity to motion of the two images necessary to construct the MTR (Fatemi et al., 2005; Smith et al., 2005). The MTCSF is the ratio between the signals obtained with the influence of an RF irradiation to produce MT contrast, $S(\Delta\omega)$, and the signal from tissue regions known to have little or no MT effect, such as CSF (when $\Delta\omega$ is greater than 1–1.5 kHz). In the case of the spinal cord, the MTCSF is calculated relative to the signal within a region of interest drawn in the CSF for each slice:

$$MTCSF(\Delta\omega) = \frac{S(\Delta\omega)}{\langle CSF \rangle_{ROI}}. \tag{3}$$

With this definition, WM is dark, GM less dark and CSF is bright. While the MTCSF does not remove dependencies on T_1 and T_2, the goal is rather to remove slice-wise variations in hardware sensitivity while maintaining information about the macromolecular protons of interest.

Both MTR and MTCSF suffer from the same drawback. Namely, they do not offer direct measurements of physiological parameters, and are sensitive to B_1 and B_0 inhomogeneity, pulse sequence parameters, T_1,

T_2, and other non-physiological contributors. Quantitative MT (qMT) is a set of analysis and acquisition methods that seek to extract quantifiable, sequence independent, values that directly reflect physiology, such as the fraction of semi-solid spins, the rate of MT exchange, or the relaxation constants of the bound spins. This approach is generally based on multiple images with varied acquisition parameters, and fitting to models to extract quantitative physiological information, and has demonstrated potential for brain imaging studies (Dortch et al., 2011, 2013; Gochberg and Gore, 2003; Sled and Pike, 2001; Smith et al., 2009; Mougin et al., 2010; Stanisz et al., 2005). To date, there have been only a few studies of qMT of the human spinal cord in vivo (Smith et al., 2009).

Post-processing and analysis methods to overcome challenges for MRI

Physiological motion

Many of the challenges of functional MRI, DTI and anatomical imaging described above have been reduced with specialized post-processing and analysis methods, using approaches that have many common features across applications. A significant source of errors arises from physiological motion either directly through physical displacements or indirectly through motion-related image artifacts; both of which introduce "noise" in time series data for fMRI, or with repeated acquisitions for DTI, MTR, etc. As this motion is naturally periodic, the choice of aperiodic stimulation paradigms for fMRI is expected to produce results that are less sensitive to this noise. Significant recent advances have also been made in methods to reduce some sources of error prior to analysis, and to account for their contributions in general linear model analyses (GLM) for both spin-echo (Figley and Stroman, 2009) and gradient-echo imaging methods (Brooks et al., 2008b; Piché et al., 2009; Stroman, 2006).

The basis functions for GLM analysis of fMRI data typically consist of models of the stimulation paradigm, convolved with the tissue response function, and low-frequency terms (Stroman et al., 2005). Models of the 3 principle components of cardiac-related motion of the spinal cord (Figley and Stroman, 2009), can be generated based on the peripheral pulse, and used as regressors in the GLM for spinal fMRI using fast spin-echo methods. For fMRI studies using gradient-echo imaging methods, signal fluctuations related to both cardiac and respiratory variations in the local magnetic field have been modeled as noise regressors in the GLM (Brooks et al., 2008a). Both the resulting basis sets can be used in the GLM analysis to reduce the variance from sources of non-interest.

Pulsatile flow of cerebrospinal fluid (CSF) has been identified as an important source of signal fluctuation through the introduction of phase errors in the k-space representation of the MRI data (Stroman et al., 2012b). These errors create an artificial displacement of CSF signal in the phase encoding direction of the resulting images, such that the CSF appears to be displaced depending on the phase of the cardiac cycle. Image correction methods have been developed to reduce the effects of this artifact (Stroman et al., 2012b).

Similarly, signal fluctuations between DTI acquisitions with different diffusion encoding directions, or different b-values, can result in significant errors in measured diffusion indices. It is therefore important to acquire DTI data in the quiescent part of the cardiac cycle, by means of peripheral gating or cardiac monitoring, with the appropriate delay set up for each case in order to perform data sampling during the diastole of the cardiac cycle (Fenyes and Narayana, 1999; Kim et al., 2007; Loy et al., 2007; Madi et al., 2005; Spuentrup et al., 2003; Summers et al., 2006). In order to reduce possible T_1 effects on the signal amplitude (i.e., T_1-induced signal variation due to variable repetition time), long repetition times should be employed when gating is used (typically TR > 5 s).

Each of these methods to correct for sources of errors and image artifacts prior to data analysis can be implemented automatically, if supporting data such as recordings of the pulse during data acquisition, are available. These methods could therefore be implemented in analysis software such as is commonly done for brain fMRI pre-processing methods, in order to make them useful in routine practice for spinal fMRI studies.

Image distortion and co-registration

Imaging methods that employ echo-planar imaging (EPI) approaches for spatial encoding are particularly sensitive to image artifacts and spatial distortion. While some fMRI approaches avoid EPI methods, many examples of fMRI in the literature, and all DTI examples, still employ EPI methods. It is highly desirable to correct these distortions if one wants to perform tractography or overlay diffusion-weighted metrics or fMRI results on distortion-free anatomical images. Various correction methods exist, and consist of estimating a non-linear warping field constrained in the phase-encoding direction. This warping field can be estimated from a magnetic field map from the phase difference between two gradient-echo images acquired at slightly different echo times (TE) (Cusack et al., 2003; Schneider and Glover, 1991; Wilson et al., 2002). This method is widely used and is implemented in software such as FSL (www.fmrib.ox.ac.uk/fsl/) and SPM (www.fil.ion.ucl.ac.uk/spm/). Another method to correct for image distortion uses an additional EPI volume acquired with the same FOV and matrix, but with phase-encoding gradients in the opposite direction. The two sets of images will exhibit distortions in the opposite direction, allowing distortion corrections to be determined (Andersson et al., 2003; Reinsberg et al., 2005; Voss et al., 2006). Effects of respiratory motion can also cause variations in local B_0-field homogeneity that result in geometric distortions that change in time and are not corrected by gating, as describe above (Brosch et al., 2002; Raj et al., 2001; Van de Moortele et al., 2002). To circumvent this issue, dynamic shimming has been proposed (van Gelderen et al., 2007). Distortion correction methods that reduce the data acquisition requirements are preferred, to avoid the cost of longer acquisitions. In addition, by reducing the EPI readout duration, the impact of susceptibility differences is decreased, thereby reducing geometrical distortions (Griswold et al., 2002; Pruessmann et al., 1999). One such approach involves using a greatly reduced field of view or ZOOM (zonally magnified oblique multi-slice) sequence (Dowell et al., 2009; Finsterbusch, 2009; Wheeler-Kingshott et al., 2002a,b). However, these methods remain largely "pre-clinical" and remain available only through research agreements with manufacturers, or as "in-house" modifications, in spite of being in use for research for over 10 years (e.g. Dowell et al., 2009; Finsterbusch and Frahm, 1999; Wheeler-Kingshott et al., 2002a; Wilm et al., 2007). Parallel imaging methods similarly reduce the data requirements, but require the availability of multi-element coils with suitable geometries that allow reduced sampling (Pruessmann et al., 1999). The gain in sampling speed however is at the expense of lower SNR and increased potential for artifacts and motion sensitivity. Most standard neck coils are not built for this purpose and consequently the benefit of parallel imaging methods for distortion correction is available only to sites with the latest or custom-built coil technology (Cohen-Adad et al., 2011c).

Motion correction

Motion correction consists of realigning all images acquired in one subject over the course of several minutes, during which time the subject may have moved. Typically for the brain, most methods consist of registering each image to a single target, which for DTI could be the b = 0 image or the average of the DW images, and for fMRI could be a high quality anatomical image, or one of the time-series image volumes. The registration is usually done by estimating an affine transformation matrix (which includes 3 rotations and 3 translations). Given that head motion is rigid (i.e., non-deformable structure) and that DW images of the brain usually contain >100,000 voxels, this procedure is usually robust and accurate. Unfortunately this does not hold for the spinal cord because (i) considerably fewer voxels are contained in the spinal cord, therefore estimating a transformation matrix might be

less robust; (ii) motion is usually non-rigid due to the segmental structure of the spine associated with swallowing, neck readjustment and B_0-variations inducing non-rigid image distortion close to the thoracic area (Brosch et al., 2002; Raj et al., 2001; Van de Moortele et al., 2002). Several techniques can help optimizing motion correction procedure for the spinal cord. With axial acquisitions, it may be advantageous to correct each slice independently, to account for the non-rigid motion of structures across slices (mainly B_0 fluctuations) (Cohen-Adad et al., 2010). In some cases it is also useful to crop the area outside the spinal region (e.g. crop out the muscles surrounding the spine) in order to optimize the accuracy of the registration in the spinal cord (Cohen-Adad et al., 2010; Summers et al., 2010). It is also possible to intersperse $b = 0$ images throughout the acquisition of the diffusion-weighted data, and then estimate the motion corrections based on the $b = 0$ images. These are typically more robust to co-align, given that all $b = 0$ images have the same contrast and have higher SNR than diffusion-weighted images. A recent detailed analysis of post-processing methods for DTI has demonstrated that slice-wise motion correction produces the most accurate results, and that in combination with eddy current correction, and robust diffusion tensor fitting methods, produces the highest contrast-to-noise ratio and least variation in FA maps (Mohammadi et al., 2013).

Positron-emission tomography (PET)

Positron emission tomography (PET) detects gamma ray emissions emitted by radioactive compounds. The choice of different injected tracers provides the potential for unique information regarding the injured spinal cord. PET imaging has at least two distinct uses in the evaluation of traumatic spinal cord injury: assessment of the metabolic activity within remaining tissue and monitoring the degree of axonal connectivity. With regard to the first use, ^{18}F-labeled fluorodeoxyglucose (FDG) has been used to monitor nervous system function in a range of preclinical and clinical studies. For example, traumatic brain injury reduces glucose utilization detected by FDG-PET, and reduced uptake is associated with impaired outcome (Garcia-Panach et al., 2011; Kato et al., 2007). This technique has also been applied to compressive and radiation myelopathies of the cervical spinal cord (Floeth et al., 2011; Uchida et al., 2004, 2009a,b) as well as to one preclinical study of traumatic spinal cord injury (Nandoe Tewarie et al., 2010). For cervical compressive myelopathies, some lesions show locally reduced glucose utilization while other cases show increased glucose uptake (Uchida et al., 2004, 2009b). There is a positive correlation between preoperatively elevated uptake and later improvement after decompressive surgery in two studies (Floeth et al., 2011; Uchida et al., 2009b). In one study, the PET data were uncorrelated with magnetic resonance (MR) images (Uchida et al., 2009b), providing a distinct means to predict positive outcome from surgery. A challenge for spinal cord PET remains spatial resolution. Even with high-resolution scanners and computed tomography (CT) registration, the spatial resolution is one or more orders of magnitude less than structural MRI. Regional distinctions between zones of the spinal cord at one segmental level are not possible by PET imaging in axial projections.

There is growing clinical trial activity focused on therapeutic strategies intended to promote axonal growth, regeneration, sprouting and repair. PET tracers with neurotransmitter specificity have the potential for tracking the degree of damage and repair for specific fiber tracts. Thus, PET ligands may function as biomarkers in the development of new repair strategies. The potential utility of this approach has been demonstrated in one preclinical study (Wang et al., 2011). The raphespinal system is the only serotonergic system in the spinal cord; therefore, all presynaptic serotonin markers depend on the continuity of descending fibers. PET tracers, such as ^{11}C-labeled 2-[2-(dimethylaminomethyl) phenylthio]-5-fluoromethylphenylamine (AFM), that bind to the presynaptic serotonin re-uptake sites have been developed (Huang et al., 2002; Williams et al., 2008; Zhu et al., 2004). In rats, the spinal cord has a clearly defined specific AFM uptake which is lost caudal to a complete spinal cord transection. With moderate spinal cord contusion, there is partial loss of caudal AFM signal. Most critically, treatment with an axon regenerative therapy, namely Nogo receptor (NgR1-Fc) decoy protein, promotes an increase in caudal AFM signal after chronic spinal cord contusion (Wang et al., 2011). This increased signal is correlated with behavioral improvement and matches post-mortem histological evidence of serotonin fiber regrowth. In this case, a neurotransmitter-specific PET tracer is a radiological marker for the extent of axonal connectivity across a lesion site and reports the degree of axonal repair with treatment. Use of tracers specific to presynaptic markers of different long tracts in the spinal cord may extend the anatomical specificity of this technique. PET measurement of fiber regrowth does not depend, as does diffusion tensor imaging (DTI)-MR measurements, on highly ordered fasciculated fiber tracts. This is critical because the majority of preclinical studies in which interventions promote some fiber regeneration show that new fiber growth is highly branched and irregular. Thus, PET may provide an imaging modality to detect regenerative growth in proof-of-concept clinical trials.

Future directions

The technical challenges common to spinal cord imaging methods have been clearly identified as being: 1) magnetic susceptibility differences, 2) physiological motion, and 3) small cross-sectional dimensions of the spinal cord. These properties of the imaging environment in the human spinal cord will not change, and so future advances require development of better methods to overcome these challenges. Improvements in imaging methods are needed to simultaneously increase the signal-to-noise ratio and the spatial resolution. For imaging methods such as PET and CT this may be obtained with improvements in detector technology, and similarly for MRI may be provided by advances in radio-frequency coil design. Improvements in MR imaging and spectroscopy methods are also needed to reduce sensitivity to magnetic field inhomogeneity. This may be achieved with improvements in localized magnetic field shimming methods, and changes in data sampling schemes to trade off shorter data sampling periods with more sampling periods. Trade-offs in image sampling are possible if pulse-sequence designs are optimized for the spinal cord environment, such as has been done for DTI (Dowell et al., 2009; Finsterbusch and Frahm, 1999; Wheeler-Kingshott et al., 2002a; Wilm et al., 2007). Such advances in methods were realized with the advent of brain fMRI, and research groups, software developers, and MRI system manufacturers responded to these demands. The future development of spinal cord imaging methods similarly requires researchers to engage with equipment manufacturers and software developers to communicate needs and encourage a two-way sharing of methods and technology. Researchers developing the methods need MRI and PET system manufacturers to make the methods more widely accessible, and in particular, accessible to clinical environments.

The future development of spinal cord imaging methods into clinical and research tools is also hindered by the relatively low number of researchers working to develop them, which results in a lack of data and technical resources. This short-fall may be alleviated by greater coordination between existing research groups and implementation of methods/processes to facilitate wide-spread sharing of methods and data. A freely accessible repository of methods, such as NITRC (http://www.nitrc.org/), could be established for spinal cord imaging software and methods, or an existing repository could be used. Similarly, methods that have already been established for sharing brain imaging data could be adopted for sharing spinal cord imaging data. Finally, but certainly not least in importance, an annual meeting dedicated to communicating results and new developments related to spinal cord imaging, is needed.

Acknowledgments

This work is the result of the efforts of the International Spinal Research Trust and the Wing for Life Spinal Cord Research Foundation to bring together researchers with a common goal of developing non-invasive imaging tools for basic and clinical spinal cord research and to support advances in treatment and rehabilitation. The goal is to speed advances and make these imaging tools more widely available by promoting collaboration between researchers and by identifying the most important challenges and needs for spinal cord imaging.

Conflict of interest statement

The authors declare that they have no financial conflicts of interest that could have an actual or perceived influence over the work presented in this paper.

References

Andersson, J.L., Skare, S., Ashburner, J., 2003. How to correct susceptibility distortions in spin-echo echo-planar images: application to diffusion tensor imaging. Neuroimage 20, 870–888.

Bammer, R., Augustin, M., Prokesch, R.W., Stollberger, R., Fazekas, F., 2002. Diffusion-weighted imaging of the spinal cord: interleaved echo-planar imaging is superior to fast spin-echo. J. Magn. Reson. Imaging 15, 364–373.

Bandettini, P.A., Wong, E.C., Jesmanowicz, A., Hinks, R.S., Hyde, J.S., 1994. Spin-echo and gradient-echo EPI of human brain activation using BOLD contrast: a comparative study at 1.5 T. NMR Biomed. 7, 12–20.

Basser, P.J., Pierpaoli, C., 1996. Microstructural and physiological features of tissues elucidated by quantitative-diffusion-tensor MRI. J. Magn. Reson. B 111, 209–219.

Beaulieu, C., 2002. The basis of anisotropic water diffusion in the nervous system — a technical review. NMR Biomed. 15, 435–455.

Brooks, J.C., Beckmann, C.F., Miller, K.L., Wise, R.G., Porro, C.A., Tracey, I., Jenkinson, M., 2008. Physiological noise modelling for spinal functional magnetic resonance imaging studies. Neuroimage 39, 680–692.

Brooks, J.C.W., Beckmann, C.F., Miller, K.L., Wise, R.G., Porro, C.A., Tracey, I., Jenkinson, M., 2008. Physiological noise modelling for spinal functional magnetic resonance imaging studies. Neuroimage 39, 680–692.

Brosch, J.R., Talavage, T.M., Ulmer, J.L., Nyenhuis, J.A., 2002. Simulation of human respiration in fMRI with a mechanical model. IEEE Trans. Biomed. Eng. 49, 700–707.

Brown, R.A., Narayanan, S., Arnold, D.L., 2012. Segmentation of magnetization transfer ratio lesions for longitudinal analysis of demyelination and remyelination in multiple sclerosis. Neuroimage 66C, 103–109.

Cercignani, M., Horsfield, M.A., Agosta, F., Filippi, M., 2003. Sensitivity-encoded diffusion tensor MR imaging of the cervical cord. AJNR Am. J. Neuroradiol. 24, 1254–1256.

Ciccarelli, O., Wheeler-Kingshott, C.A., McLean, M.A., Cercignani, M., Wimpey, K., Miller, D.H., Thompson, A.J., 2007. Spinal cord spectroscopy and diffusion-based tractography to assess acute disability in multiple sclerosis. Brain 130, 2220–2231.

Ciccarelli, O., Toosy, A.T., De Stefano, N., Wheeler-Kingshott, C.A., Miller, D.H., Thompson, A.J., 2010. Assessing neuronal metabolism in vivo by modeling imaging measures. J. Neurosci. 30 (45), 15030–15033.

Clark, C.A., Barker, G.J., Tofts, P.S., 2000. Improved reduction of motion artifacts in diffusion imaging using navigator echoes and velocity compensation. J. Magn. Reson. 142, 358–363.

Cohen-Adad, J., Benali, H., Hoge, R.D., Rossignol, S., 2008. In vivo DTI of the healthy and injured cat spinal cord at high spatial and angular resolution. Neuroimage 40, 685–697.

Cohen-Adad, J., Lundell, H., Rossignol, S., 2009. Distortion correction in spinal cord DTI: what's the best approach? Proceedings of the 17th Annual Meeting of ISMRM, Honolulu, USA, p. 3178.

Cohen-Adad, J., Gauthier, C.J., Brooks, J.C.W., Slessarev, M., Han, J., Fisher, J.A., Rossignol, S., Hoge, R.D., 2010. BOLD signal responses to controlled hypercapnia in human spinal cord. Neuroimage 50, 1074–1084.

Cohen-Adad, J., El Mendili, M.-M., Lehéricy, S., Pradat, P.-F., Blancho, S., Rossignol, S., Benali, H., 2011. Demyelination and degeneration in the injured human spinal cord detected with diffusion and magnetization transfer MRI. Neuroimage 55, 1024–1033.

Cohen-Adad, J., Leblond, H., Delivet-Mongrain, H., Martinez, M., Benali, H., Rossignol, S., 2011. Wallerian degeneration after spinal cord lesions in cats detected with diffusion tensor imaging. Neuroimage 57, 1068–1076.

Cohen-Adad, J., Mareyam, A., Keil, B., Polimeni, J.R., Wald, L.L., 2011. 32-channel RF coil optimized for brain and cervical spinal cord at 3 T. Magn. Reson. Med. 66, 1198–1208.

Cooke, F.J., Blamire, A.M., Manners, D.N., Styles, P., Rajagopalan, B., 2004. Quantitative proton magnetic resonance spectroscopy of the cervical spinal cord. Magn. Reson. Med. 51, 1122–1128.

Cusack, R., Brett, M., Osswald, K., 2003. An evaluation of the use of magnetic field maps to undistort echo-planar images. Neuroimage 18, 127–142.

Dortch, R.D., Li, K., Gochberg, D.F., Welch, E.B., Dula, A.N., Tamhane, A.A., Gore, J.C., Smith, S.A., 2011. Quantitative magnetization transfer imaging in human brain at 3 T via selective inversion recovery. Magn. Reson. Med. 66, 1346–1352.

Dortch, R.D., Moore, J., Li, K., Jankiewicz, M., Gochberg, D.F., Hirtle, J.A., Gore, J.C., Smith, S.A., 2013. Quantitative magnetization transfer imaging of human brain at 7 T. Neuroimage 64, 640–649.

Dowell, N.G., Jenkins, T.M., Ciccarelli, O., Miller, D.H., Wheeler-Kingshott, C.A., 2009. Contiguous-slice zonally oblique multislice (CO-ZOOM) diffusion tensor imaging: examples of in vivo spinal cord and optic nerve applications. J. Magn. Reson. Imaging 29, 454–460.

Edden, R.A., Bonekamp, D., Smith, M.A., Dubey, P., Barker, P.B., 2007. Proton MR spectroscopic imaging of the medulla and cervical spinal cord. Magn. Reson. Imaging 26 (4), 1101–1105.

Ellingson, B.M., Ulmer, J.L., Kurpad, S.N., Schmit, B.D., 2008. Diffusion tensor MR imaging in chronic spinal cord injury. AJNR Am. J. Neuroradiol. 29, 1976–1982.

Elliott, J.M., Pedler, A.R., Cowin, G., Sterling, M., McMahon, K., 2012. Spinal cord metabolism and muscle water diffusion in whiplash. Spinal Cord 50, 474–476.

Elshafiey, I., Bilgen, M., He, R., Narayana, P.A., 2002. In vivo diffusion tensor imaging of rat spinal cord at 7 T. Magn. Reson. Imaging 20, 243–247.

Fatemi, A., Smith, S.A., Dubey, P., Zackowski, K.M., Bastian, A.J., van Zijl, P.C., Moser, H.W., Raymond, G.V., Golay, X., 2005. Magnetization transfer MRI demonstrates spinal cord abnormalities in adrenomyeloneuropathy. Neurology 64, 1739–1745.

Feinberg, D.A., Mark, A.S., 1987. Human brain motion and cerebrospinal fluid circulation demonstrated with MR velocity imaging. Radiology 163, 793–799.

Fenyes, D.A., Narayana, P.A., 1999. In vivo diffusion characteristics of rat spinal cord. Magn. Reson. Imaging 17, 717–722.

Figley, C.R., Stroman, P.W., 2006. Characterization of spinal cord motion: a source of errors in spinal fMRI? Proceedings of the International Society for Magnetic Resonance in Medicine 14th Annual Meeting, Seattle, Washington, May 4–9, 2006.

Figley, C.R., Stroman, P.W., 2007. Investigation of human cervical and upper thoracic spinal cord motion: implications for imaging spinal cord structure and function. Magn. Reson. Med. 58, 185–189.

Figley, C.R., Stroman, P.W., 2009. Development and validation of retrospective spinal cord motion time-course estimates (RESPITE) for spin-echo spinal fMRI: improved sensitivity and specificity by means of a motion-compensating general linear model analysis. Neuroimage 44, 421–427.

Figley, C.R., Stroman, P.W., 2011. The role(s) of astrocytes and astrocyte activity in neurometabolism, neurovascular coupling, and the production of functional neuroimaging signals. Eur. J. Neurosci. 33, 577–588.

Figley, C.R., Leitch, J.K., Stroman, P.W., 2010. In contrast to BOLD: signal enhancement by extravascular water protons as an alternative mechanism of endogenous fMRI signal change. Magn. Reson. Imaging 28, 1234–1243.

Finsterbusch, J., 2009. High-resolution diffusion tensor imaging with inner field-of-view EPI. J. Magn. Reson. Imaging 29, 987–993.

Finsterbusch, J., Frahm, J., 1999. Single-shot line scan imaging using stimulated echoes. J. Magn. Reson. 137, 144–153.

Floeth, F.W., Stoffels, G., Herdmann, J., Eicker, S., Galldiks, N., Rhee, S., Steiger, H.J., Langen, K.J., 2011. Prognostic value of 18F-FDG PET in monosegmental stenosis and myelopathy of the cervical spinal cord. J. Nucl. Med. 52, 1385–1391.

Garcia-Panach, J., Lull, N., Lull, J.J., Ferri, J., Martinez, C., Sopena, P., Robles, M., Chirivella, J., Noe, E., 2011. A voxel-based analysis of FDG-PET in traumatic brain injury: regional metabolism and relationship between the thalamus and cortical areas. J. Neurotrauma 28, 1707–1717.

Gati, J.S., Menon, R.S., Ugurbil, K., Rutt, B.K., 1997. Experimental determination of the BOLD field strength dependence in vessels and tissue. Magn. Reson. Med. 38, 296–302.

Gochberg, D.F., Gore, J.C., 2003. Quantitative imaging of magnetization transfer using an inversion recovery sequence. Magn. Reson. Med. 49, 501–505.

Gomez-Anson, B., MacManus, D.G., Parker, G.J., et al., 2000. In vivo 1H-magnetic resonance spectroscopy of the spinal cord in humans. Neuroradiology 42, 515–517.

Goto, N., Otsuka, N., 1997. Development and anatomy of the spinal cord. Neuropathology 17, 25–31.

Graham, S.J., Henkelman, R.M., 1997. Understanding pulsed magnetization transfer. J. Magn. Reson. Imaging 7, 903–912.

Griswold, M.A., Jakob, P.M., Heidemann, R.M., Nittka, M., Jellus, V., Wang, J., Kiefer, B., Haase, A., 2002. Generalized autocalibrating partially parallel acquisitions (GRAPPA). Magn. Reson. Med. 47, 1202–1210.

Gulani, V., Iwamoto, G.A., Jiang, H., Shimony, J.S., Webb, A.G., Lauterbur, P.C., 1997. A multiple echo pulse sequence for diffusion tensor imaging and its application in excised rat spinal cords. Magn. Reson. Med. 38, 868–873.

Gullapalli, J., Krejza, J., Schwartz, E.D., 2006. In vivo DTI evaluation of white matter tracts in rat spinal cord. J. Magn. Reson. Imaging 24, 231–234.

Heidemann, R.M., Ozsarlak, O., Parizel, P.M., Michiels, J., Kiefer, B., Jellus, V., Müller, M., Breuer, F., Blaimer, M., Griswold, M.A., Jakob, P.M., 2003. A brief review of parallel magnetic resonance imaging. Eur. Radiol. 13, 2323–2337.

Henkelman, R.M., Stanisz, G.J., Graham, S.J., 2001. Magnetization transfer in MRI: a review. NMR Biomed. 14, 57–64.

Henning, A., Schär, M., Kollias, S.S., Boesiger, P., Dydak, U., 2008. Quantitative magnetic resonance spectroscopy in the entire human cervical spinal cord and beyond at 3T. Magn. Reson. Med. 59 (6), 1250–1258.

Holder, C.A., Muthupillai, R., Mukundan, S., Eastwood, J.D., Hudgins, P.A., 2000. Diffusion-weighted MR imaging of the normal human spinal cord in vivo. AJNR Am. J. Neuroradiol. 21, 1799–1806.

Holly, L.T., Freitas, B., McArthur, D.L., Salamon, N., 2009. Proton magnetic resonance spectroscopy to evaluate spinal cord axonal injury in cervical spondylotic myelopathy. J. Neurosurg. Spine 10, 194–200.

Horsfield, M.A., Jones, D.K., 2002. Applications of diffusion-weighted and diffusion tensor MRI to white matter diseases — a review. NMR Biomed. 15, 570–577.

Huang, Y., Hwang, D.R., Narendran, R., Sudo, Y., Chatterjee, R., Bae, S.A., Mawlawi, O., Kegeles, L.S., Wilson, A.A., Kung, H.F., Laruelle, M., 2002. Comparative evaluation

in nonhuman primates of five PET radiotracers for imaging the serotonin transporters: [11C]McN 5652, [11C]ADAM, [11C]DASB, [11C]DAPA, and [11C]AFM. J. Cereb. Blood Flow Metab. 22, 1377–1398.
Jeong, E.K., Kim, S.E., Guo, J., Kholmovski, E.G., Parker, D.L., 2005. High-resolution DTI with 2D interleaved multislice reduced FOV single-shot diffusion-weighted EPI (2D ss-rFOV-DWEPI). Magn. Reson. Med. 54, 1575–1579.
Jochimsen, T.H., Norris, D.G., Moller, H.E., 2005. Is there a change in water proton density associated with functional magnetic resonance imaging? Magn. Reson. Med. 53, 470–473.
Jones, D.K., 2004. The effect of gradient sampling schemes on measures derived from diffusion tensor MRI: a Monte Carlo study. Magn. Reson. Med. 51, 807–815.
Jones, D.K., Horsfield, M.A., Simmons, A., 1999. Optimal strategies for measuring diffusion in anisotropic systems by magnetic resonance imaging. Magn. Reson. Med. 42, 515–525.
Jones, D.K., Williams, S.C., Gasston, D., Horsfield, M.A., Simmons, A., Howard, R., 2002. Isotropic resolution diffusion tensor imaging with whole brain acquisition in a clinically acceptable time. Hum. Brain Mapp. 15, 216–230.
Jones, C.K., Xiang, Q.S., Whittall, K.P., MacKay, A.L., 2004. Linear combination of multiecho data: short T2 component selection. Magn. Reson. Med. 51, 495–502.
Kachramanoglou, C., De Vita, E., Thomas, D.L., Wheeler-Kingshott, C.A., Balteau, E., Carlstedt, T., Choi, D., Thompson, A.J., Ciccarelli, O., 2013. Metabolic changes in the spinal cord after brachial plexus root re-implantation. Neurorehabil. Neural Repair 27, 118–124.
Kato, T., Nakayama, N., Yasokawa, Y., Okumura, A., Shinoda, J., Iwama, T., 2007. Statistical image analysis of cerebral glucose metabolism in patients with cognitive impairment following diffuse traumatic brain injury. J. Neurotrauma 24, 919–926.
Kendi, A.T., Tan, F.U., Kendi, M., Yilmaz, S., Huvaj, S., Tellioğlu, S., 2004. MR spectroscopy of cervical spinal cord in patients with multiple sclerosis. Neuroradiology 46 (9), 764–769.
Kharbanda, H.S., Alsop, D.C., Anderson, A.W., Filardo, G., Hackney, D.B., 2006. Effects of cord motion on diffusion imaging of the spinal cord. Magn. Reson. Med. 56, 334–339.
Kim, J.H., Loy, D.N., Liang, H.F., Trinkaus, K., Schmidt, R.E., Song, S.K., 2007. Noninvasive diffusion tensor imaging of evolving white matter pathology in a mouse model of acute spinal cord injury. Magn. Reson. Med. 58, 253–260.
Klawiter, E.C., Schmidt, R.E., Trinkaus, K., Liang, H.F., Budde, M.D., Naismith, R.T., Song, S.K., Cross, A.H., Benzinger, T.L., 2011. Radial diffusivity predicts demyelination in ex vivo multiple sclerosis spinal cords. Neuroimage 55, 1454–1460.
Laule, C., Leung, E., Lis, D.K., Traboulsee, A.L., Paty, D.W., MacKay, A.L., Moore, G.R., 2006. Myelin water imaging in multiple sclerosis: quantitative correlations with histopathology. Mult. Scler. 12, 747–753.
Laule, C., Vavasour, I.M., Zhao, Y., Traboulsee, A.L., Oger, J., Vavasour, J.D., Mackay, A.L., Li, D.K., 2010. Two-year study of cervical cord volume and myelin water in primary progressive multiple sclerosis. Mult. Scler. 16, 670–677.
Lin, C.S., Fertikh, D., Davis, B., Lauerman, W.C., Henderson, F., Schellinger, D., 2000. 2D CSI proton MR spectroscopy of human spinal vertebra: feasibility studies. J. Magn. Reson. Imaging 11, 287–293.
Lindberg, P.G., Feydy, A., Maier, M.A., 2010. White matter organization in cervical spinal cord relates differently to age and control of grip force in healthy subjects. J. Neurosci. 30, 4102–4109.
Loy, D.N., Kim, J.H., Xie, M., Schmidt, R.E., Trinkaus, K., Song, S.K., 2007. Diffusion tensor imaging predicts hyperacute spinal cord injury severity. J. Neurotrauma 24, 979–990.
MacMillan, E.L., Madler, B., Fichtner, N., Dvorak, M.F., Li, D.K., Curt, A., MacKay, A.L., 2011. Myelin water and T(2) relaxation measurements in the healthy cervical spinal cord at 3.0 T: repeatability and changes with age. Neuroimage 54, 1083–1090.
Madi, S., Hasan, K.M., Narayana, P.A., 2005. Diffusion tensor imaging of in vivo and excised rat spinal cord at 7 T with an icosahedral encoding scheme. Magn. Reson. Med. 53, 118–125.
Marliani, A.F., Clementi, V., Albini-Riccioli, L., Agati, R., Leonardi, M., 2007. Quantitative proton magnetic resonance spectroscopy of the human cervical spinal cord at 3 Tesla. Magn. Reson. Med. 57 (1), 160–163.
Marliani, A.F., Clementi, V., Albini Riccioli, L., Agati, R., Carpenzano, M., Salvi, F., Leonardi, M., 2010. Quantitative cervical spinal cord 3T proton MR spectroscopy in multiple sclerosis. AJNR Am. J. Neuroradiol. 31, 180–184.
Matsuzaki, H., Wakabayashi, K., Ishihara, K., Ishikawa, H., Kawabata, H., Onomura, T., 1996. The origin and significance of spinal cord pulsation. Spinal Cord 34, 422–426.
McCreary, C.R., Bjarnason, T.A., Skihar, V., Mitchell, J.R., Yong, V.W., Dunn, J.F., 2009. Multiexponential T2 and magnetization transfer MRI of demyelination and remyelination in murine spinal cord. Neuroimage 45, 1173–1182.
Moffett, J.R., Ross, B., Arun, P., Madhavarao, C.N., Namboodiri, A.M., 2007. N-Acetylaspartate in the CNS: from neurodiagnostics to neurobiology. Prog. Neurobiol. 81, 89–131.
Mohamed, F.B., Hunter, L.N., Barakat, N., Liu, C.-S.J., Sair, H., Samdani, A.F., Betz, R.R., Faro, S.H., Gaughan, J., Mulcahey, M.J., 2011. Diffusion tensor imaging of the pediatric spinal cord at 1.5 T: preliminary results. AJNR Am. J. Neuroradiol. 32, 339–345.
Mohammadi, S., Freund, P., Feiweier, T., Curt, A., Weiskopf, N., 2013. The impact of post-processing on spinal cord diffusion tensor imaging. Neuroimage 70, 377–385.
Mougin, O.E., Coxon, R.C., Pitiot, A., Gowland, P.A., 2010. Magnetization transfer phenomenon in the human brain at 7 T. Neuroimage 49, 272–281.
Murphy, K., Bodurka, J., Bandettini, P.A., 2007. How long to scan? The relationship between fMRI temporal signal to noise ratio and necessary scan duration. Neuroimage 34, 565–574.
Nandoe Tewarie, R.D., Yu, J., Seidel, J., Rahiem, S.T., Hurtado, A., Tsui, B.M., Grotenhuis, J.A., Pomper, M.G., Oudega, M., 2010. Positron emission tomography for serial imaging of the contused adult rat spinal cord. Mol. Imaging 9, 108–116.
Nevo, U., Hauben, E., Yoles, E., Agranov, E., Akselrod, S., Schwartz, M., Neeman, M., 2001. Diffusion anisotropy MRI for quantitative assessment of recovery in injured rat spinal cord. Magn. Reson. Med. 45, 1–9.
Nunes, R.G., Jezzard, P., Behrens, T.E., Clare, S., 2005. Self-navigated multishot echo-planar pulse sequence for high-resolution diffusion-weighted imaging. Magn. Reson. Med. 53, 1474–1478.
Ohgiya, Y., Oka, M., Hiwatashi, A., Liu, X., Kakimoto, N., Westesson, P.L., Ekholm, S.E., 2007. Diffusion tensor MR imaging of the cervical spinal cord in patients with multiple sclerosis. Eur. Radiol. 17, 2499–2504.
Onu, M., Gervai, P., Cohen-Adad, J., Lawrence, J., Kornelsen, J., Tomanek, B., Sboto-Frankenstein, U.N., 2010. Human cervical spinal cord funiculi: investigation with magnetic resonance diffusion tensor imaging. J. Magn. Reson. Imaging 31, 829–837.
Piché, M., Cohen-Adad, J., Nejad, M.K., Perlbarg, V., Xie, G., Beaudoin, G., Benali, H., Rainville, P., 2009. Characterization of cardiac-related noise in fMRI of the cervical spinal cord. Magn. Reson. Imaging 27, 300–310.
Pruessmann, K.P., Weiger, M., Scheidegger, M.B., Boesiger, P., 1999. SENSE: sensitivity encoding for fast MRI. Magn. Reson. Med. 42, 952–962.
Qian, W., Chan, Q., Mak, H., Zhang, Z., Anthony, M.-P., Yau, K.K.-W., Khong, P.-L., Chan, K.H., Kim, M., 2011. Quantitative assessment of the cervical spinal cord damage in neuromyelitis optica using diffusion tensor imaging at 3 Tesla. J. Magn. Reson. Imaging 33, 1312–1320.
Raj, D., Anderson, A.W., Gore, J.C., 2001. Respiratory effects in human functional magnetic resonance imaging due to bulk susceptibility changes. Phys. Med. Biol. 46, 3331–3340.
Reinsberg, S.A., Doran, S.J., Charles-Edwards, E.M., Leach, M.O., 2005. A complete distortion correction for MR images: II. Rectification of static-field inhomogeneities by similarity-based profile mapping. Phys. Med. Biol. 50, 2651–2661.
Schmierer, K., Scaravilli, F., Altmann, D.R., Barker, G.J., Miller, D.H., 2004. Magnetization transfer ratio and myelin in postmortem multiple sclerosis brain. Ann. Neurol. 56, 407–415.
Schmierer, K., Tozer, D.J., Scaravilli, F., Altmann, D.R., Barker, G.J., Tofts, P.S., Miller, D.H., 2007. Quantitative magnetization transfer imaging in postmortem multiple sclerosis brain. J. Magn. Reson. Imaging 26, 41–51.
Schneider, E., Glover, G., 1991. Rapid in vivo proton shimming. Magn. Reson. Med. 18, 335–347.
Schwartz, E.D., Yezierski, R.P., Pattany, P.M., Quencer, R.M., Weaver, R.G., 1999. Diffusion-weighted MR imaging in a rat model of syringomyelia after excitotoxic spinal cord injury. AJNR Am. J. Neuroradiol. 20, 1422–1428.
Schwartz, E.D., Chin, C.L., Shumsky, J.S., Jawad, A.F., Brown, B.K., Wehrli, S., Tessler, A., Murray, M., Hackney, D.B., 2005. Apparent diffusion coefficients in spinal cord transplants and surrounding white matter correlate with degree of axonal dieback after injury in rats. AJNR Am. J. Neuroradiol. 26, 7–18.
Shen, H., Tang, Y., Huang, L., Yang, R., Wu, Y., Wang, P., Shi, Y., He, X., Liu, H., Ye, J., 2007. Applications of diffusion-weighted MRI in thoracic spinal cord injury without radiographic abnormality. Int. Orthop. 31, 375–383.
Sled, J.G., Pike, G.B., 2000. Quantitative interpretation of magnetization transfer in spoiled gradient echo MRI sequences. J. Magn. Reson. 145, 24–36.
Sled, J.G., Pike, G.B., 2001. Quantitative imaging of magnetization transfer exchange and relaxation properties in vivo using MRI. Magn. Reson. Med. 46, 923–931.
Smith, S.A., Golay, X., Fatemi, A., Jones, C.K., Raymond, G.V., Moser, H.W., van Zijl, P.C., 2005. Magnetization transfer weighted imaging in the upper cervical spinal cord using cerebrospinal fluid as intersubject normalization reference (MTCSF imaging). Magn. Reson. Med. 54, 201–206.
Smith, S.A., Farrell, J.A., Jones, C.K., Reich, D.S., Calabresi, P.A., van Zijl, P.C., 2006. Pulsed magnetization transfer imaging with body coil transmission at 3 Tesla: feasibility and application. Magn. Reson. Med. 56, 866–875.
Smith, S.A., Edden, R.A., Farrell, J.A., Barker, P.B., van Zijl, P.C., 2008. Measurement of T1 and T2 in the cervical spinal cord at 3 Tesla. Magn. Reson. Med. 60, 213–219.
Smith, S.A., Golay, X., Fatemi, A., Mahmood, A., Raymond, G.V., Moser, H.W., van Zijl, P.C., Stanisz, G.J., 2009. Quantitative magnetization transfer characteristics of the human cervical spinal cord in vivo: application to adrenomyeloneuropathy. Magn. Reson. Med. 61, 22–27.
Smith, S.A., Jones, C.K., Gifford, A., Belegu, V., Chodkowski, B., Farrell, J.A.D., Landman, B.A., Reich, D.S., Calabresi, P.A., McDonald, J.W., Van Zijl, P.C.M., 2010. Reproducibility of tract-specific magnetization transfer and diffusion tensor imaging in the cervical spinal cord at 3 Tesla. NMR Biomed. 23, 207–217.
Spuentrup, E., Buecker, A., Koelker, C., Guenther, R.W., Stuber, M., 2003. Respiratory motion artifact suppression in diffusion-weighted MR imaging of the spine. Eur. Radiol. 13, 330–336.
Stanisz, G.J., Odrobina, E.E., Pun, J., Escaravage, M., Graham, S.J., Bronskill, M.J., Henkelman, R.M., 2005. T1, T2 relaxation and magnetization transfer in tissue at 3 T. Magn. Reson. Med. 54, 507–512.
Stejskal, E.O., Tanner, J.E., 1965. Spin diffusion measurements: spin echoes in the presence of a time-dependent field gradient. J. Phys. Chem. 42, 288–292.
Stroman, P.W., 2006. Discrimination of errors from neuronal activity in functional MRI of the human spinal cord by means of general linear model analysis. Magn. Reson. Med. 56, 452–456.
Stroman, P.W., 2010. Creating an image from the magnetic resonance signal. In: Han, L. (Ed.), Essentials of Functional MRI. CRC Press, Taylor & Francis Group, Boca Raton, FL, pp. 97–120.
Stroman, P.W., Ryner, L.N., 2001. Functional MRI of motor and sensory activation in the human spinal cord. Magn. Reson. Imaging 19, 27–32.
Stroman, P.W., Krause, V., Frankenstein, U.N., Malisza, K.L., Tomanek, B., 2001. Spin-echo versus gradient-echo fMRI with short echo times. Magn. Reson. Imaging 19, 827–831.
Stroman, P.W., Krause, V., Malisza, K.L., Frankenstein, U.N., Tomanek, B., 2001. Characterization of contrast changes in functional MRI of the human spinal cord at 1.5 T. Magn. Reson. Imaging 19, 833–838.

Stroman, P.W., Krause, V., Malisza, K.L., Frankenstein, U.N., Tomanek, B., 2002. Extravascular proton-density changes as a non-BOLD component of contrast in fMRI of the human spinal cord. Magn. Reson. Med. 48, 122–127.
Stroman, P.W., Malisza, K.L., Onu, M., 2003. Functional magnetic resonance imaging at 0.2 Tesla. Neuroimage 20, 1210–1214.
Stroman, P.W., Tomanek, B., Krause, V., Frankenstein, U.N., Malisza, K.L., 2003. Functional magnetic resonance imaging of the human brain based on signal enhancement by extravascular protons (SEEP fMRI). Magn. Reson. Med. 49, 433–439.
Stroman, P.W., Kornelsen, J., Lawrence, J., Malisza, K.L., 2005. Functional magnetic resonance imaging based on SEEP contrast: response function and anatomical specificity. Magn. Reson. Imaging 23, 843–850.
Stroman, P.W., Lee, A.S., Pitchers, K.K., Andrew, R.D., 2008. Magnetic resonance imaging of neuronal and glial swelling as an indicator of function in cerebral tissue slices. Magn. Reson. Med. 59, 700–706.
Stroman, P.W., Bosma, R.L., Beynon, M., Dobek, C., 2012. Test–retest reliability of spinal cord fMRI in healthy participants. 20th Annual Meeting of International Society for Magnetic Resonance in Medicine, Melbourne, Australia.
Stroman, P.W., Bosma, R.L., Beynon, M., Dobek, C., 2012. Removal of synergistic physiological motion and image artefacts in functional MRI of the human spinal cord. 20th Annual Meeting of the International Society for Magnetic Resonance in Medicine, Melbourne, Australia.
Summers, P., Staempfli, P., Jaermann, T., Kwiecinski, S., Kollias, S., 2006. A preliminary study of the effects of trigger timing on diffusion tensor imaging of the human spinal cord. AJNR Am. J. Neuroradiol. 27, 1952–1961.
Summers, P.E., Ferraro, D., Duzzi, D., Lui, F., Iannetti, G.D., Porro, C.A., 2010. A quantitative comparison of BOLD fMRI responses to noxious and innocuous stimuli in the human spinal cord. Neuroimage 50, 1408–1415.
Thron, A.K., 1988. Vascular Anatomy of the Spinal Cord: Neurological Investigations and Clinical Syndromes. Springer-Verlag, New York 8–64.
Thurnher, M.M., Bammer, R., 2006. Diffusion-weighted MR imaging (DWI) in spinal cord ischemia. Neuroradiology 48, 795–801.
Uchida, K., Kobayashi, S., Yayama, T., Kokubo, Y., Nakajima, H., Kakuyama, M., Sadato, N., Tsuchida, T., Yonekura, Y., Baba, H., 2004. Metabolic neuroimaging of the cervical spinal cord in patients with compressive myelopathy: a high-resolution positron emission tomography study. J. Neurosurg. Spine 1, 72–79.
Uchida, K., Nakajima, H., Takamura, T., Kobayashi, S., Tsuchida, T., Okazawa, H., Baba, H., 2009. Neurological improvement associated with resolution of irradiation-induced myelopathy: serial magnetic resonance imaging and positron emission tomography findings. J. Neuroimaging 19, 274–276.
Uchida, K., Nakajima, H., Yayama, T., Kobayashi, S., Shimada, S., Tsuchida, T., Okazawa, H., Mwaka, E., Baba, H., 2009. High-resolution magnetic resonance imaging and 18FDG-PET findings of the cervical spinal cord before and after decompressive surgery in patients with compressive myelopathy. Spine (Phila Pa 1976) 34, 1185–1191.
Van de Moortele, P.F., Pfeuffer, J., Glover, G.H., Ugurbil, K., Hu, X., 2002. Respiration-induced B0 fluctuations and their spatial distribution in the human brain at 7 Tesla. Magn. Reson. Med. 47, 888–895.
van Gelderen, P., de Zwart, J.A., Starewicz, P., Hinks, R.S., Duyn, J.H., 2007. Real-time shimming to compensate for respiration-induced B0 fluctuations. Magn. Reson. Med. 57, 362–368.
Van Hecke, W., Leemans, A., Sijbers, J., Vandervliet, E., Van Goethem, J., Parizel, P.M., 2008. A tracking-based diffusion tensor imaging segmentation method for the detection of diffusion-related changes of the cervical spinal cord with aging. J. Magn. Reson. Imaging 27, 978–991.
Voss, H.U., Watts, R., Uluğ, A.M., Ballon, D., 2006. Fiber tracking in the cervical spine and inferior brain regions with reversed gradient diffusion tensor imaging. Magn. Reson. Imaging 24, 231–239.
Wang, X., Duffy, P., McGee, A.W., Hasan, O., Gould, G., Tu, N., Harel, N.Y., Huang, Y., Carson, R.E., Weinzimmer, D., Ropchan, J., Benowitz, L.I., Cafferty, W.B., Strittmatter, S.M., 2011. Recovery from chronic spinal cord contusion after Nogo receptor intervention. Ann. Neurol. 70, 805–821.
Wheeler-Kingshott, C.A., Hickman, S.J., Parker, G.J., Ciccarelli, O., Symms, M.R., Miller, D.H., Barker, G.J., 2002. Investigating cervical spinal cord structure using axial diffusion tensor imaging. Neuroimage 16, 93–102.
Wheeler-Kingshott, C.A., Parker, G.J., Symms, M.R., Hickman, S.J., Tofts, P.S., Miller, D.H., Barker, G.J., 2002. ADC mapping of the human optic nerve: increased resolution, coverage, and reliability with CSF-suppressed ZOOM-EPI. Magn. Reson. Med. 47, 24–31.
Whittall, K.P., MacKay, A.L., Graeb, D.A., Nugent, R.A., Li, D.K., Paty, D.W., 1997. In vivo measurement of T2 distributions and water contents in normal human brain. Magn. Reson. Med. 37, 34–43.
Williams, W.A., Neumeister, A., Nabulsi, N., Ropchan, J., Labaree, D., Planeta-Wilson, B., Najafzadeh, S., Carson, R.E., Huang, Y., 2008. First in human evaluation of [11C] AFM, a novel PET tracer for the serotonin transporter. Neuroimage 41, T42-T42.
Wilm, B.J., Svensson, J., Henning, A., Pruessmann, K.P., Boesiger, P., Kollias, S.S., 2007. Reduced field-of-view MRI using outer volume suppression for spinal cord diffusion imaging. Magn. Reson. Med. 57, 625–630.
Wilm, B.J., Gamper, U., Henning, A., Pruessmann, K.P., Kollias, S.S., Boesiger, P., 2009. Diffusion-weighted imaging of the entire spinal cord. NMR Biomed. 22, 174–181.
Wilson, J.L., Jenkinson, M., de Araujo, I., Kringelbach, M.L., Rolls, E.T., Jezzard, P., 2002. Fast, fully automated global and local magnetic field optimization for fMRI of the human brain. Neuroimage 17, 967–976.
Wolff, S.D., Balaban, R.S., 1989. Magnetization transfer contrast (MTC) and tissue water proton relaxation in vivo. Magn. Reson. Med. 10, 135–144.
Wu, Y., Alexander, A.L., Fleming, J.O., Duncan, I.D., Field, A.S., 2006. Myelin water fraction in human cervical spinal cord in vivo. J. Comput. Assist. Tomogr. 30, 304–306.
Zhu, Z., Guo, N., Narendran, R., Erritzoe, D., Ekelund, J., Hwang, D.R., Bae, S.A., Laruelle, M., Huang, Y., 2004. The new PET imaging agent [11C]AFE is a selective serotonin transporter ligand with fast brain uptake kinetics. Nucl. Med. Biol. 31, 983–994.